A broadband waveguide for protein crystallography under intense microwave fields

R. Weissenborn
Universität Konstanz, Fachbereich Physik, 78457 Konstanz, Germany

T. Reinhardt and V. Hansen
Bergische Universität Wuppertal, Fachbereich Elektrotechnik und Informationstechnik, 42097 Wuppertal, Germany

G. Maret and T. Gisler[a)]
Universität Konstanz, Fachbereich Physik, 78457 Konstanz, Germany

(Received 14 April 2004; accepted 26 July 2004; published 15 November 2004)

We present a slab-line waveguide whose geometry is optimized for wide-angle x-ray diffraction (XRD) experiments on protein crystals during irradiation with intense microwave fields. Characterization of the waveguide transmission and reflectivity (using time-domain reflectometry) and of the electric field distribution inside the waveguide (using finite-difference time-domain calculations) shows that the present device has a broad bandwidth from below 0.5 to 18 GHz, allowing one to perform frequency-dependent XRD studies with a well-defined transverse mode structure and negligible reflection losses. As shown with a specific example, our device provides a simple way to couple microwave irradiation experiments with high-resolution x-ray diffraction measurements from millimeter-size crystalline samples. The present design might prove useful for systematic studies of microwave effects on protein structure and dynamics. © *2004 American Institute of Physics.* [DOI: 10.1063/1.1813771]

I. INTRODUCTION

Investigating the interaction of microwave fields with biological systems at the molecular level could help one to understand the response of cells and entire organisms to microwave fields such as emitted by mobile phone antennas. The present literature on microwave effects on biological systems is extensive and contradictory.[1] In particular, experiments designed to probe nonthermal microwave effects (i.e., effects not related to microwave-induced heating of water) occurring in narrow frequency windows have seldom been repeated by independent research groups. In the few examples of repeated experiments, nonthermal microwave effects could not be reproduced.

On the other hand, detailed molecular mechanisms of nonthermal absorption of microwave radiation by proteins and nucleic acids have not been identified to date. Low-frequency intramolecular vibrations of proteins and nucleic acids have long been discussed as possible channels into which microwave energy could be deposited nonthermally. It has however been argued by Adair[2] that the resonant excitation of such vibrational modes by a microwave field should be absent if realistic viscous damping by the surrounding water shell is taken into account. Nevertheless, the analysis of Adair is schematic, neglecting the strong anharmonicity of the interactions in proteins and the strong ordering of the water on the surface of the protein molecule.[3]

A sensitive method to directly identify nonthermal effects of microwave radiation on proteins is x-ray diffraction (XRD). Wide-angle XRD data from single protein crystals can be analyzed to yield the average positions and mean-squared displacements with atomic resolution. Nonthermal effects of microwave radiation should thus appear as atomic displacement and mobility patterns different from the ones obtained by mere heating of the crystal when the XRD experiment is performed under simultaneous irradiation with microwaves.

Typically, high-quality protein single crystals can be grown in sizes of at most 1–2 mm. This precludes the use of focused free-space Gaussian microwave beams delivered by horn antennas since most of the emitted power would not hit the protein crystal. This situation is only slightly improved when conventional microwave resonators are used. However, a well-defined mode structure and **E**-field distribution is paid by a narrow bandwidth for resonant operation. Slab-line waveguides (a variant of coaxial lines), on the other hand, allow one to concentrate the **E** field in a small localized region and, besides, have a much wider bandwidth than resonators, making them more suitable for frequency sweeping experiments. Both resonators and slab-line waveguides, however, impose severe geometrical constraints for wide-angle x-ray diffraction experiments.

In this work we present a broadband microwave waveguide based on a slab-line geometry which allows one to record wide-angle x-ray diffractograms from small protein crystals exposed to intense microwave fields with a well-defined distribution of the electric field strength. Finite-difference time-domain calculations are performed in order to determine the electric field distribution inside the wave-

[a)]Electronic mail: thomas.gisler@uni-konstanz.de

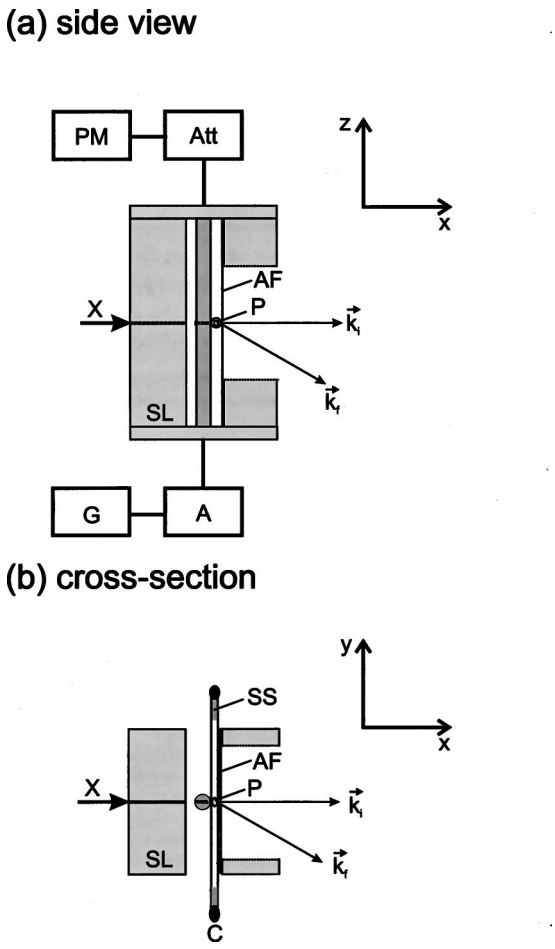

FIG. 1. Side view (a) and cross-sectional view (b) of the slab-line waveguide modified for wide-angle x-ray diffraction under microwave irradiation. G: microwave generator, A: amplifier, SL: slab-line, P: protein crystal, AF: aluminum foil, X: x-ray beam, Att: attenuator, PM: power meter, C: capillary, SS: salt solution. $\mathbf{k}_i$ and $\mathbf{k}_f$ are the wave vectors of primary and diffracted beams, respectively.

guide, and the waveguide is characterized experimentally by time-domain reflectometry. We present examples of the performance of the device for the structure determination of proteins.

II. LAYOUT OF MICROWAVE WAVEGUIDE

The waveguide is a modification of a slab-line waveguide, consisting of two parallel aluminum plates separated by a distance $D=5.5$ mm and a central conductor made out of a cylindrical brass rod with a diameter $d=3$ mm (see Fig. 1). Inner and outer conductors were connected to *N*-type flanges.

In order to allow for wide-angle XRD experiments one of the outer plates was replaced by an aluminum frame onto which an aluminum foil with a thickness $\delta=20$ μm was mounted. This thickness is much larger than the Skin depth $\delta_{\mathrm{Skin}}=(\pi\mu\mu_0\nu\sigma)^{-1/2}$ (Ref. 4) in Al, which is between 2.6 and 0.61 μm for frequencies between $\nu=1$ GHz and $\nu=18$ GHz [using a permeability $\mu=1.000\,02$ and the specific conductivity $\sigma=3.77\times10^7\ \Omega^{-1}\,\mathrm{m}^{-1}$ for Al at $T=293$ K (Ref. 5)]. This allows the electromagnetic field to be guided with negligible loss, while still allowing diffracted x-ray light to reach the detector with only slight attenuation by the aluminum foil.

In a typical experiment the protein crystal (mounted in a thin quartz glass capillary to avoid dehydration) is placed in the 1.25-mm-wide gap between the inner conductor and the Al foil where the **E**-field strength has its maximum (see Fig. 1). The primary x-ray beam directed along the *x* axis perpendicular to the axis of the waveguide then illuminates the sample through a small bore 0.7 mm in diameter drilled through the center of the inner conductor and the massive outer conductor plate. Diffracted x-ray beams propagate through the Al foil onto the image plate detector. In order to avoid diffraction signals from the Al foil the latter is punctured in order to allow unobstructed passage of the primary beam.

For XRD under simultaneous microwave irradiation we use single-frequency continuous-wave signals generated by a swept signal generator (Micro-Tel Corporation SG-811B); after amplification by a traveling-wave tube amplifier (Varian 6991K3) to a power $P\leqslant20$ W the signal is coupled into the waveguide. For lack of space the amplifier output line is connected to the waveguide by an angle connector. The transmitted power is attenuated and directed into a power meter (Hewlett-Packard 432A with power sensor 8478B).

III. WAVEGUIDE CHARACTERIZATION

For a conventional slab-line geometry, the impedance Z is related to the separation between the two outer conductors, D, and the diameter d of the inner conductor by the expression $Z=(1/2\pi)\sqrt{\mu\mu_0/(\epsilon\epsilon_0)}\ln(4D/\pi d)=50\ \Omega$.[6] Using a network analyzer we measure an impedance $Z=52.1\ \Omega$ at 0.5 GHz for the unmodified slab-line waveguide. This value is consistent with the result of a numerical finite-difference time-domain (FDTD) calculation[7] which yields $Z=50.19\ \Omega$ at $\nu=2$ GHz. This calculation also yields the complete electric field distribution for the fundamental transverse mode shown in Fig. 2. The electric field of the fundamental mode is found to be highly localized in the narrow gap between the inner and outer conductor [Fig. 2(a)]. In the region of maximal field strength the field points radially outwards from the center of the inner conductor [see Fig. 2(b)]. In the *y* direction, perpendicular to the waveguide axis, the field strength decays rapidly within a distance of about 3 mm, which is considerably smaller than the width $w=30$ mm of the outer conductor. This result is consistent with the experimentally observed absence of stray fields outside the slab-line.

Scattering of the fundamental transverse mode by the bores in the modified slab-line could lead to the excitation of higher-order modes which no longer have their maximal field strength in the gap between inner and outer conductors. The bores should then appear as impedance mismatches inside the waveguide, which can be detected by time-domain reflectometry. Using a digital sampling oscilloscope (Tektronix 11801) we have thus measured the time-resolved reflectivity $r(t)$ as a function of the pulse travel time t (see Fig. 3). For these measurements the waveguide was terminated by 50 Ω at its exit. The impedance $Z(s)$ as a function of the position

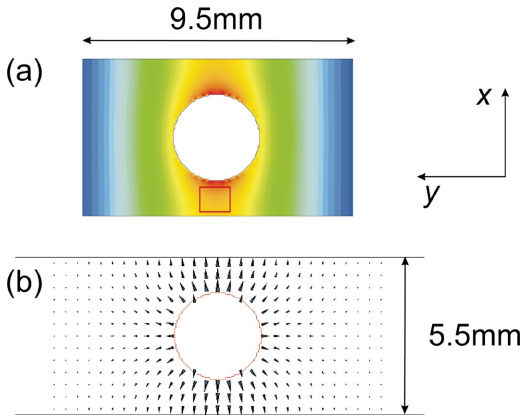

FIG. 2. (Color) Magnitude (a) and direction (b) of the microwave **E** field inside the waveguide near the inner conductor determined with a finite-difference time-domain (FDTD) calculation at $\nu=2$ GHz. The calculation was performed with a maximal resolution at the surface of the inner conductor of 0.48 mm in the z direction and 0.05 mm in the x and y directions. In (a) the code ranges from low field strength to high field strength. The protein crystal is placed at the position of maximum field strength marked by the red rectangle. Here the field intensity is 0.12 W/mm^2 for 1 W input power at $\nu=2$ GHz, calculated by FDTD under the assumption of perfect impedance matching. This intensity corresponds to an **E**-field amplitude of 9.5 kV/m.

$s=ct/2$ in the waveguide was then computed using the relation $Z(s)=Z_w(1+r(t))/(1-r(t))$, where $Z_w=50\ \Omega$ is the impedance of the coaxial line to the waveguide[8] and c is the speed of light in vacuum; we assumed a dielectric constant $\epsilon=1$ throughout the transmission line. The presence of a 90° N-type angle connector at the transition between the coaxial cable and the waveguide leads to a strong reflection ($Z\approx 64\ \Omega$). The connectors of the waveguide at $s=4.5$ cm and at $s=8$ cm give rise to weak mismatches ($Z\approx 53\ \Omega$). In turn, the part of the waveguide between the connectors is well matched with the coaxial line, as shown by the weak structure of $Z(s)$ in this region.

In order to test whether the presence of the bore through the central conductor affects the impedance of the waveguide, we measured $Z(s)$ with the bore aligned along the y and along the x axes. The latter configuration is used for the XRD experiments. When the bore is oriented along the x axis, the disturbance of the electric field is expected to be maximal. However, the experiment only shows a slightly increased value of $Z(s)$ in that position, indicating that the disturbance of the electric field distribution due to the bore is negligible.

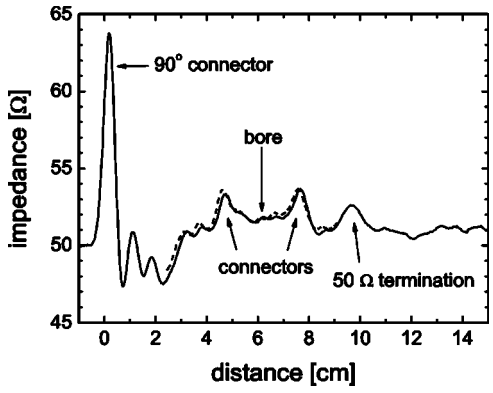

FIG. 3. Dependence of the impedance $Z(s)$ on the distance s in the waveguide, determined from the measured time-dependent reflectivity $r(t)$ of a modified slab-line waveguide. The bore through the inner conductor allowing the passage of the primary x-ray beam is aligned along the y direction (dashed line) and along the x direction (full line) which is the orientation used in the XRD experiments.

The presence of a strong microwave field was checked by measuring microwave-induced Brillouin scattering from a piezoelectrical quartz crystal:[9,10] we placed a small ($1\times 1\times 2$ mm^3) x-cut quartz crystal in the position of maximal field strength between inner and outer conductor. The crystal was then illuminated by a coherent laser beam at a wavelength $\lambda_L=532$ nm along the y direction, and light scattered in near-forward direction at a scattering angle $\vartheta=8.4°$ was analyzed with a tandem Fabry–Pérot interferometer[11] and detected by a photomultiplier. Near-forward scattering was chosen to match the directions of **E** field and scattering wave vector **q**.[12] At this wave vector the Brillouin spectrum shows a longitudinal acoustic (LA) phonon line at $\Delta\nu_B=2.5$ GHz. In the presence of the microwave field at $\nu=2.45$ GHz a sharp line at the microwave frequency rises out of the thermal Brillouin spectrum. This signal originates from Brillouin scattering from LA phonons induced by piezoelectric coupling of the microwave field to the crystal lattice. For 30 W microwave input power we obtain an increase of the Brillouin signal by a factor of 300 beyond the thermal signal. Similar, albeit smaller induced Brillouin signals were also obtained in backscattering geometry, where now the condition of mode-matching ($\mathbf{E}\|\mathbf{q}$) has been relaxed.

IV. X-RAY DIFFRACTION FROM PROTEIN CRYSTALS IN THE WAVEGUIDE

Figure 4(a) shows an x-ray diffraction pattern from a single crystal of hen-egg white (HEW) lysozyme placed in the waveguide, recorded at a wavelength $\lambda=1.54$ Å with a MAR 345 image plate detector with a diameter of 24 cm. At this wavelength the mass attenuation coefficient of Al is $\mu'(\lambda)=48.500$ cm^2/g,[13] leading to an angle-dependent transmission for the diffracted x-ray beams $T(\theta)=e^{-\mu'(\lambda)\rho_m\delta/\cos\theta}$, where $\rho_m=2.72$ g/cm^3 is the density of Al. The scattering angle θ is the angle between incident wave vector $\mathbf{k}_i$ and diffracted wave vector $\mathbf{k}_f$. At the maximal diffraction angle $\theta=45°$ the transmission was thus $T(\theta)=0.69$. Without correction for the angle-dependent attenuation the presence of the Al foil shows up as an increased Wilson B-factor B_W. In our test experiments on lysozyme single crystals we measured $B_W=25.1$ Å^2 for a crystal outside the waveguide and $B_W=27.1$ Å^2 for the same crystal placed in the waveguide. In the analysis of the diffractograms using the program XDS[14] the attenuation can be accounted for by performing the extinction correction for all diffraction spots using a fictitious increased air pressure.

We have used this new method to record complete diffraction data sets under simultaneous microwave irradiation at 8 GHz and high power levels from tetragonal HEW lysozyme single crystals. These experiments yield detailed insight into microwave-caused changes of structure and

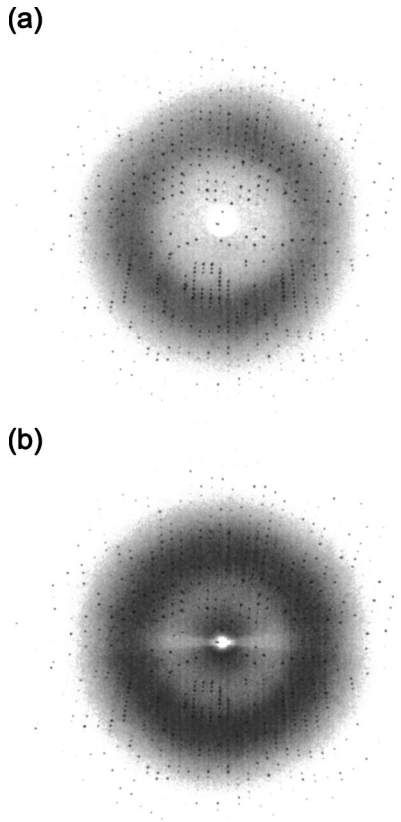

FIG. 4. X-ray diffraction patterns from a tetragonal hen-egg white lysozyme single crystal placed in the waveguide (a) and outside the waveguide (b). At the sample–detector distance of 12 cm the maximal scattering angle $\theta = 45°$ corresponds to a resolution of 2.0 Å. The dark halo is due to x-ray scattering from water.

mean-square displacements on the atomic scale. Details about these experiments will be given in a separate publication.

ACKNOWLEDGMENTS

The authors thank R. Kremer and H. R. Benedickter for experimental support, K. Dransfeld and M. Lehndorff for helpful discussions, and K. Diederichs for help with the XRD data analysis. This work was funded by the Optik-Zentrum Konstanz.

[1] E. Postow and M. L. Swicord, in *Handbook of Biological Effects of Electromagnetic Fields*, edited by C. Polk and E. Postow (CRC Press, Boca Raton, 1996), pp. 535–580.
[2] R. K. Adair, Biophys. J. **82**, 1147 (2002).
[3] S. C. Harvey and P. Hoekstra, J. Phys. Chem. **76**, 2987 (1972).
[4] J. D. Jackson, *Classical Electrodynamics*, 2nd ed. (Wiley, New York, 1975).
[5] *CRC Handbook of Chemistry and Physics*, 80th ed., edited by D. R. Lide (CRC Press, Boca Raton, FL, 1999).
[6] M. A. R. Gunston, *Microwave Transition Line Impedance Data*, 2nd ed. (Nobel, 1997).
[7] A. Taflove and S. C. Hagness, *Computational Electrodynamics: The Finite-Difference Time-Domain Method* (Artech House, Boston, 2000).
[8] G. Käs and P. Pauli, *Mikrowellentechnik: Grundlagen, Anwendung, Messtechnik* (Franzis, München, 1991).
[9] J. Krüger and H.-G. Unruh, Solid State Commun. **21**, 583 (1977).
[10] H. Sussner and R. Vacher, Appl. Opt. **18**, 3815 (1979).
[11] S. M. Lindsay, M. W. Anderson, and J. R. Sandercock, Rev. Sci. Instrum. **52**, 1478 (1981).
[12] D. Sommer, W. Kleemann, M. Lehndorff, and K. Dransfeld, Solid State Commun. **72**, 731 (1989).
[13] J. H. Hubbell, Int. J. Appl. Radiat. Isot. **33**, 1269 (1982).
[14] W. Kabsch, in *Crystallography of Biological Macromolecules*, edited by M. G. Rossmann and E. Arnold, International Tables for Crystallography, Vol. F (Kluwer, Dordrecht, 2001), pp. 218–225.